a_{om} = frequency ratio at resonance;
B = foundation halfwidth;
b = mass ratio (Eq. 5);
C_p, C_s = P- and S-wave velocities of soil;
C_r = S-wave velocity of rock;
F_v = vertical compliance (displacement) function;
$f_{1,v}, f_{2,v}$ = real and imaginary parts of F_v (Eq. 3b);
G = shear modulus;
h = ω/C_p = P-wave number;
k = ω/C_s = S-wave number;
M = total mass of foundation, per unit length;
m_e = total unbalanced mass of rotating machine, per unit length;
P, P_o = exciting force and its amplitude, per unit length;
$P(\xi)$ = Fourier Transform of $p(x)$ (Eq. 6);
$p(x)$ = harmonic line traction acting at point x on free surface;
R = total soil reaction, per unit length;
r = radius of circular foundations (Eq. 15);
$U(\xi)$ = Fourier Transform of u or w (Eq. 10);
u, w = horizontal and vertical displacements;
β = critical damping ratio of the soil;
δ, δ_o = vertical displacement of foundation and its amplitude (Fig. 2);
$\bar{\delta}_o$ = dimensionless amplitude of vertical displacement (Eq. 4);
σ, τ = normal and shear stresses;
ψ = phase angle; and
ω = frequency of vibration, in radians per second.

JOURNAL OF THE GEOTECHNICAL ENGINEERING DIVISION

SHEAR AND RAYLEIGH WAVES IN SOIL DYNAMICS

By George Gazetas,[1] A. M. ASCE and Mishac K. Yegian,[2] M. ASCE

INTRODUCTION

Ground surface motions recorded during earthquakes reflect, to some degree, the seismic characteristics of the underlying soil layers at the recording site (15,16). In geotechnical earthquake engineering this influence of the local site conditions upon the stresses and motion within a soil profile often needs to be evaluated, e.g., in the design of nuclear power plants the design motion is commonly specified at the free surface, and then estimates of compatible motions are made at a number of specified depths [Fig. 1(a)]. Similarly, to estimate the ground-failure potential at a site by liquefaction of loose, saturated sand layers, it is necessary to compute the earthquake-induced shear stresses in these layers from a design earthquake motion specified either at bedrock or at the ground surface [Fig. 1(b)]. Furthermore, to describe the motion at site A, the accelerogram recorded at second site B must be properly modified (both in intensity and frequency content) to account for the effect of local soil conditions [Fig. 1(c)].

Current procedures that are commonly used to study these problems are based on an assumption of vertically propagating shear waves (S-waves). This assumption has been employed because it is difficult, if not impossible, to accurately predict the nature of incoming waves for a potential earthquake and because it leads to simple analytical solutions. Furthermore, it is known that for motions close to the epicenter, continuous transmission of upward propagating S-waves through increasingly soft soil layers gradually changes their direction of propagation to nearly vertical, as is schematically depicted in Fig. 2.

Recent studies give evidence of significant participation of surface waves in recorded motions (1,4,8,9,13,19,21,22,23). In addition, it has been suggested (4,11) that surface waves may induce motions and stresses in the foundation soils different from those calculated based on the assumption of vertical S-waves.

Note.—Discussion open until May 1, 1980. To extend the closing date one month, a written request must be filed with the Editor of Technical Publications, ASCE. This paper is part of the copyrighted Journal of the Geotechnical Engineering Division, Proceedings of the American Society of Civil Engineers, Vol. 105, No. GT12, December, 1979. Manuscript was submitted for review for possible publication on June 7, 1979.

[1] Asst. Prof. of Civ. Engrg., Case Western Reserve Univ., Cleveland, Ohio.
[2] Asst. Prof. of Civ. Engrg., Northeastern Univ., Boston, Mass.

Furthermore, the assumption of vertical S-waves has been criticized since it leads to excessive deamplification with depth. These criticisms have prompted the research reported herein, which investigates the influence of Rayleigh (R) and shear (S) wave propagation upon computed variation of motions with depth.

This paper first reviews the published evidence concerning the presence of R-waves in recorded motions used in earthquake engineering practice and then presents a brief description of the wave propagation theory used in this study. Finally, results are presented comparing the computed (elastic) responses of typical soil profiles due to several harmonic R-waves and S-waves of given periods.

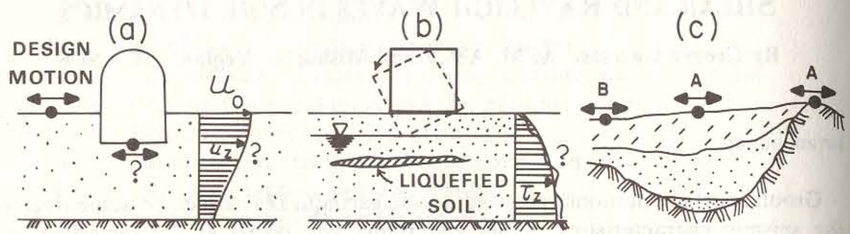

FIG. 1.—Typical Applications of Wave Propagation Theories to Soil Dynamics Problems

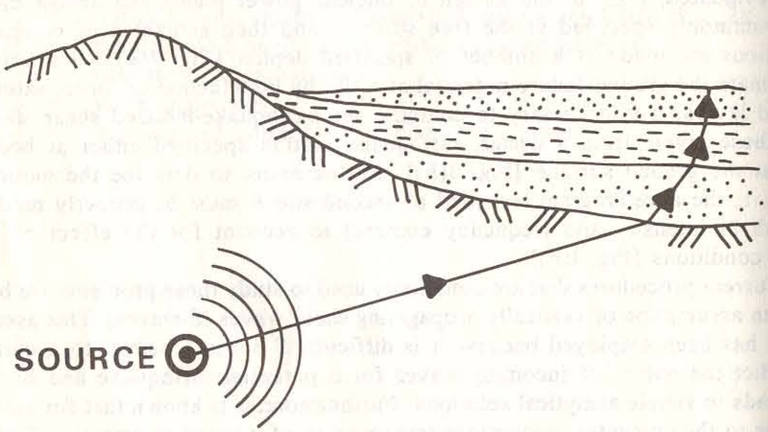

FIG. 2.—Change of Direction of Wave Propagation to Near Vertical due to Transmission through Increasingly Soft Layers

Evidence of R-Waves in Recorded Motions

Until recently, it was believed that R-waves appeared only at very large distances (several hundred kilometers or more) from the earthquake source, and were therefore of little interest to engineers. However, a number of studies published in the last few years have seriously undermined this belief, demonstrating that surface waves actually play a significant role in the production of strong ground motions, even in the "near field," during shallow-focused earthquakes.

For example, Trifunac (22), in an attempt to explain some of the 1971 San Fernando earthquake records, concluded that body-wave dislocation theory fails to "predict" the later portions of the accelerograms, especially at long distances from the source, and suggested that surface waves should also be considered. Anderson (1) drew a similar conclusion for the Parkfield earthquake of 1966, while Hermann and Nuttli (8) developed a multimode surface wave theory that seems to successfully explain recorded ground motions with periods longer than 1.5 sec at distances greater than 100 km from the source. Such motions may cause damage to tall buildings or offshore structures.

Toki (21), using dispersion techniques, was able to disintegrate strong motion accelerograms recorded during the San Fernando Earthquake into surface and body waves, and concluded that while the first 6 sec–8 sec of motion are mainly due to body waves, R-waves contribute significantly to the remaining portion of the records.

Similarly, Liang and Duke (9) presented a method to separate body and surface wave contents in strong-motion accelerograms using source-to-site transfer function of the motion for two recording stations where the Fourier transforms of the accelerograms are known. They conclude that even for motions recorded at distances less than 20 km from the epicenter, the contribution of surface waves may be important.

More recently, Swanger and Boore (19) constructed synthetic accelerograms by superposition of surface-wave modes and compared them with recorded motions. They concluded that

> for shallow sources in typical earth structures, surface waves dominate the ground motion at moderate distances, on the order of tens of kms, and at periods greater than 1 or 2 sec.

Finally, Trifunac (23), studying the amplitude attenuation with distance of 187 motions (recorded during 57 earthquakes), attributed the change in the slope of the attenuation curve at a distance of 75 km to the "slower attenuation of surface waves with distance and the fact that in this distance range, surface waves emerge as the main contributors to strong shaking."

The writers feel that although further research is needed to increase the reliability of some of the aforementioned methods and additional data are required to substantiate their conclusions, there is clear evidence of the presence of surface waves at distances on the order of 50 km or greater.

Nakamo (as reported in Ref. 3) suggested that minimum epicentral distance R required for the first appearance of R-waves in a homogeneous medium is given by

$$R \geq \frac{h}{\left[\left(\frac{c_P}{c_R}\right)^2 - 1\right]^{1/2}} \quad \text{. . . . . (1)}$$

in which c_P and c_R = the dilatational (P) and R-wave velocities, respectively; and h = the focal depth. Thus, for an average value of the ratio c_P/c_R = 2 (corresponding to a Poisson's ratio $\nu \simeq 0.30$), the minimum distance before

R-waves can appear is equal to approx $0.6h$. Thus, R-waves will be present at distances that are of interest to earthquake engineers, excluding cases in which the focal depth is very large (on the order of hundreds of kilometers).

Theory of S-Wave and R-Wave Propagation

In horizontally stratified soils in which the individual layers are characterized by linearly elastic and homogeneous properties, wave propagation can be studied using the method developed by Thomson (20) and Haskell (7). (Since R-waves are of importance in moderate and long epicentral distances, the assumption of elastic soil response seems realistic except, perhaps, with unusually strong earthquakes.)

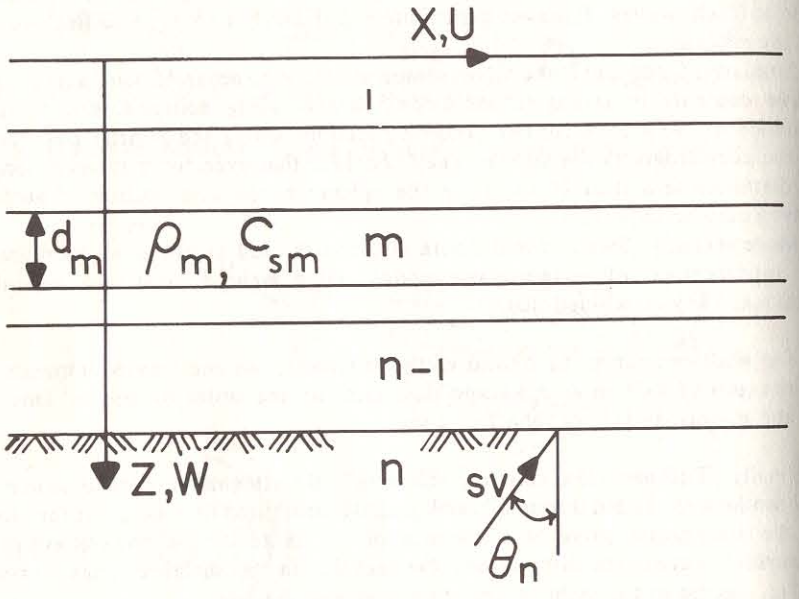

FIG. 3.—Soil Geometry and Coordinate Axes

Consider the soil system shown in Fig. 3. The general harmonic solution of the wave equations for the mth layer can be expressed in terms of dilation and rotation, i.e.

$$\epsilon_m \equiv \frac{\partial u}{\partial x} + \frac{\partial w}{\partial z};$$

$$\epsilon_m = \exp\,[i(\omega t - kx)]\,[A'_m \exp\,(-ik\alpha_m z) + A''_m \exp\,(ik\alpha_m z)] \quad \ldots\ldots\ldots (2a)$$

$$\Omega_m \equiv \frac{1}{2}\left(\frac{\partial u}{\partial z} - \frac{\partial w}{\partial x}\right);$$

$$\Omega_m = \exp\,[i(\omega t - kx)]\,[B'_m \exp\,(-ik\beta_m z) + B''_m \exp\,(ik\beta_m z)] \quad \ldots\ldots\ldots (2b)$$

in which $k = \omega/c$ = the apparent wave number in the x direction; c = the horizontal phase velocity, common for all the layers; $\alpha_m = [(c/c_{Pm})^2 - 1]^{1/2}$; $\beta_m = [(c/c_{sm})^2 - 1]^{1/2}$ (where c_{Pm} and c_{sm} = the P and S wave velocities of the mth layer); and A'_m, A''_m, B'_m, and B''_m are constants. The term with A'_m, for example, represents a plane P-wave whose direction of propagation forms an angle arc cos α_m with $+z$ direction if α_m is real or a wave propagating in the $+x$ direction with amplitude exponentially decaying in the $+z$ direction if α_m is imaginary. The same applies for the term with A''_m, if $-z$ is substituted for $+z$, while B'_m, B''_m correspond to rotational waves.

Eqs. 2*a* and 2*b* apply for both S-waves and R-waves. The boundary conditions at the free surface and at the $n-1$ layer interfaces are also identical for both types of waves. At the free surface, normal and shear stresses must vanish at all times, due to lack of exciting surface sources:

$$\sigma_1(x, 0; t) = \tau_1(x, 0; t) = 0 \quad \ldots\ldots\ldots (3)$$

while at any layer interface, continuity of displacement and stresses must be preserved:

$$\sigma_{m-1}(x, z_m; t) = \sigma_m(x, z_m; t); \quad \tau_{m-1}(x, z_m; t) = \tau_m(x, z_m; t);$$

$$u_{m-1}(x, z_m; t) = u_m(x, z_m; t); \quad w_{m-1}(x, z_m; t) = w_m(x, z_m; t);$$

$$(m = 2, \ldots, n) \quad \ldots\ldots\ldots (4)$$

Stresses and displacements can be derived from Eqs. 2*a* and 2*b* using the equations of linear elasticity (e.g., Ref. 7).

Eqs. 3 and 4 provide $4n - 2$ equations to determine the $4n$ constants A'_m, A''_m, B'_m, and $B''_m (m = 1, \ldots, n)$. Therefore, two more boundary conditions that will account for the nature of the propagating waves are necessary.

S-Waves.—In this case, the constants A''_n, B''_n can easily be determined from amplitude a_{sn} and direction θ_n of the incident S-wave, which is traveling up from infinity (see Fig. 3):

$$A''_n = 0; \quad B''_n = \left(\frac{\omega}{2c_{sn}}\right) a_{sn} \quad \ldots\ldots\ldots (5)$$

while the phase velocity is given by

$$c = \frac{c_{sn}}{\sin\theta_n} \quad \ldots\ldots\ldots (6)$$

Thus, the $4n$ constants A', A'', B', and B'' among the $4n$ equations (Eqs. 3, 4, and 5) can be eliminated, and displacements and stresses at any depth can be expressed in terms of amplitude a_{sn} and direction cosine cos θ_n of the incident S-wave. Alternatively, displacement attenuation and stress distribution with depth can be determined as functions of the horizontal motion (displacement or acceleration) at the free surface for any particular angle of incidence of the S-wave.

For the characteristic case of a homogeneous elastic soil deposit underlain by an elastic halfspace (simulating rock), the attenuation with depth of the horizontal motion in the deposit due to a vertically propagating S-wave (SV-wave) is

$$U_s \equiv \frac{u_s(z)}{u_s(0)} = \cos\left(\frac{\omega z}{c_s}\right) = \cos\left(2\pi \frac{z}{\lambda_s}\right) \quad \ldots\ldots\ldots\ldots\ldots\ldots (7)$$

in which $u_s(0)$ and $u_s(z)$ = the amplitudes of motion at ground surface and at depth z, respectively; c_s = the shear wave velocity of the soil; and λ_s = the wave length. Note that ratio of displacements U_s is independent of the subsurface conditions existing below elevation z under consideration. This is generally true for any number of layers when vertical shear waves are considered but is not true for R-waves unless their wave length, λ_R, is less than approx $z/2$.

R-Waves.—They are "surface" waves and therefore have no source(s) at infinite depth. Thus

$$A_n'' = B_n'' = 0 \quad \ldots\ldots\ldots\ldots\ldots\ldots\ldots\ldots\ldots\ldots\ldots\ldots (8)$$

and the boundary relationships lead to a linear homogeneous algebraic system of $4n - 2$ equations in $4n - 2$ unknowns, of the form

$$[J]\{D\} = 0 \quad \ldots\ldots\ldots\ldots\ldots\ldots\ldots\ldots\ldots\ldots\ldots\ldots (9)$$

in which $\{D\} = \{A_1', B_1', A_1'', B_1'', \ldots, A_n', B_n'\}^T$ = the vector of the unknown constants; and $[J]$ = a matrix whose elements are functions of phase velocity c and wave frequency ω for a given soil profile.

Nontrivial solutions of $\{D\}$ exist only if the determinant of the coefficient matrix vanishes. Thus, for any given ω, the so-called "period" equation

$$[J] = 0 \quad \ldots\ldots\ldots\ldots\ldots\ldots\ldots\ldots\ldots\ldots\ldots\ldots (10)$$

defines the possible phase velocities for R-waves in a stratified medium. Solution vectors $\{D\}$ of Eq. 9 that correspond to acceptable phase velocities c are the eigenvectors or R-wave modes of the particular stratified soil deposit at the wave frequency considered. Normalized with respect to horizontal displacement at the free surface, each mode represents the attenuation of motion with depth due to passage of an R-wave consisting exclusively of this mode.

The numerical technique of Haskell (7) and Harkrider (6), properly modified to treat shallow and soft soil layers in addition to deep-stiff earth zones that are of interest in seismology, was implemented to determine the eigenvalues and eigenvectors of the soil profiles studied in this paper. However, only attenuation functions due to the fundamental Rayleigh mode are reported here, and these functions are compared with the distribution of dynamic displacements with depth due to S-waves.

A characteristic case is that of the propagation of R-waves along the surface of a halfspace. Only one wave mode is possible for any particular frequency, and velocity c varies between approx 0.92 c_s and 0.95 c_s for values of Poisson ratio ν between 0.25 and 0.50, respectively (3). The soil particles that are forced to move horizontally and vertically follow an elliptical path, with vertical major and horizontal minor principal axes. The attenuations of the horizontal (u_R) and vertical (w_R) components of motion with depth when $\nu = 0.25$ are

$$U_R \equiv \frac{u_R(z)}{u_R(0)} = 2.40\left[\exp\left(-5.34\frac{z}{\lambda}\right) - 0.58\exp\left(-2.45\frac{z}{\lambda}\right)\right] \quad \ldots\ldots (11a)$$

$$\text{and} \quad W_R \equiv \frac{w_R(z)}{w_R(0)} = 1.64\left[0.85\exp\left(-5.34\frac{z}{\lambda}\right) - 1.46\exp\left(-2.45\frac{z}{\lambda}\right)\right] \quad \ldots\ldots\ldots\ldots\ldots\ldots\ldots\ldots (11b)$$

while $w_R(0)/u_R(0) \simeq 1.5$.

Fig. 4(*a*) compares U_R (from Eq. 11*a*) with U_s (from Eq. 7). It is clear that the two attenuation curves are fundamentally different. The R-waves excite only a "small" upper part of the halfspace and the motions are significant only up to a depth of the order of a wavelength or less, contrary to S-waves, that propagate vertically upward and excite essentially the "whole" halfspace

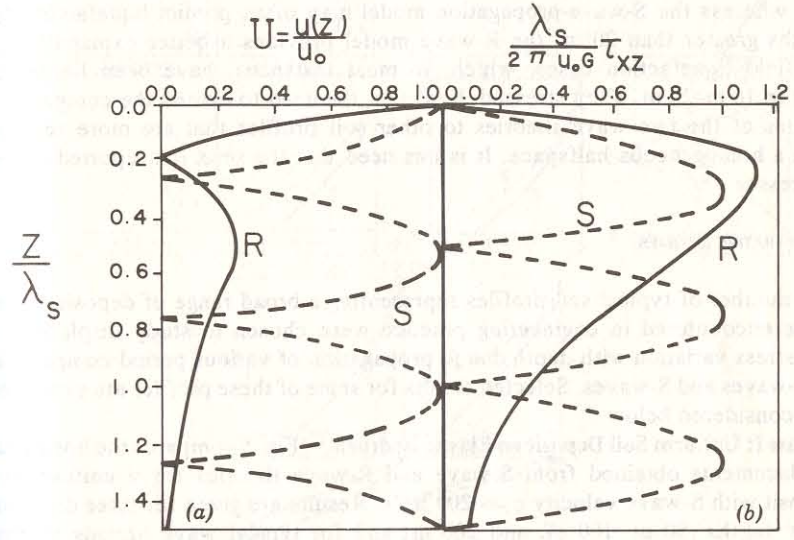

FIG. 4.—Vertical S- and R-Waves Propagating in Halfspace: (*a*) Displacements; (*b*) Shear Stresses

despite the observed null points at depths equal to odd multiples of quarter wavelengths $\lambda/4$.

A similar conclusion is drawn from a comparison of horizontal shear stresses τ_{xz} on horizontal planes. In a dimensionless form, the variation of shear stresses with depth for S-waves and R-waves and $\nu = 0.25$ is given, respectively, by

$$\frac{\lambda}{2\pi u_0 G}\tau_{xz}^S = \sin\left(2\pi\frac{z}{\lambda}\right) \quad \ldots\ldots\ldots\ldots\ldots\ldots\ldots\ldots (12a)$$

$$\text{and} \quad \frac{\lambda}{2\pi u_0 G}\tau_{xz}^R = 4\left[\exp\left(-2.45\frac{z}{\lambda}\right) - \exp\left(-5.34\frac{z}{\lambda}\right)\right] \quad \ldots\ldots (12b)$$

in which τ_{xz}^S and τ_{xz}^R = the horizontal shear stresses from S-waves and R-waves, respectively; u_0 = the amplitude of motion at ground surface; and G = the

shear modulus of the soil. The two variations are depicted in Fig. 4(*b*), where it is again observed that R-waves excite only the upper part of the halfspace and then rapidly attenuate at depths larger than a wavelength, contrary to S-waves that excite the entire halfspace. However, it is interesting to note that near the ground surface the R-wave-induced shear stresses are about one and one-half to two times as large as those induced by the vertical S-wave. For higher values of Poisson's ratio, the R-wave-induced stresses would be even higher (approx three times the S-wave stresses for $\nu = 0.45$). The importance of this result to the liquefaction potential of a soil deposit has been considered in some detail by Hall, et al. (5). Studying the variation with depth of stress-reduction factor $r_d(z)$, which Seed and Idriss (18) used in simplified analyses for liquefaction, they argued that, "it decreases much more rapidly with depth for the Rayleigh-wave model than it does for the shear-wave model." Hall, et al. (5) have argued that whereas the S-wave-propagation model may often predict liquefaction for depths greater than 20 m, the R-wave model provides a better explanation of the field liquefaction cases, which, in most instances, have been limited to the top 10 m–20 m. They stressed, however, the need to extend the comparative studies of the two wave theories to other soil profiles that are more realistic than a homogeneous halfspace. It is this need that the research reported herein addresses.

Comparative Studies

A number of typical soil profiles representing a broad range of deposits likely to be encountered in engineering practice were chosen to study displacement and stress variation with depth due to propagation of various period components of R-waves and S-waves. Selected results for some of these profiles are presented and considered below.

Case I: Uniform Soil Deposit on Elastic Bedrock.—Fig. 5 compares the horizontal displacements obtained from S-wave and R-wave theories for a uniform soil deposit with S-wave velocity $c_s = 200$ m/s. Results are given for three different layer depths (50 m, 100 m, and 200 m) and for typical wave periods ranging from 1 sec–4 sec. Fundamental S-wave natural periods T_s of the three deposits are 1 sec, 2 sec, and 4 sec, respectively.

As shown in Fig. 5, S-waves and R-waves produce similar variations of displacements with depth throughout the period range studied. This agreement is particularly good for long periods, beyond the fundamental period of the deposits, T_s. For example, the differences between the two waves at periods larger than 3 sec in the 100-m deposit are negligibly small [Fig. 5(*b*)]. At periods around T_s some differences are observed, but they are essentially restricted to the lower part of the deposit and would therefore be of no significance in most engineering applications. However, well below the fundamental period of a deposit, the discrepancies between the two wave predictions become significant. At such periods the wavelengths (λ_S or λ_R) are much shorter than depth H of the deposit. Thus, since R-waves propagate along the surface and decay at depths of approx $1.5\lambda_R$, they essentially do not "see" the bedrock at very short periods. Consequently, they are not influenced by its presence, and the resulting attenuation of motions with depth tends to be the same as that in a halfspace. Vertical S-waves, however, excite the entire deposit, resulting

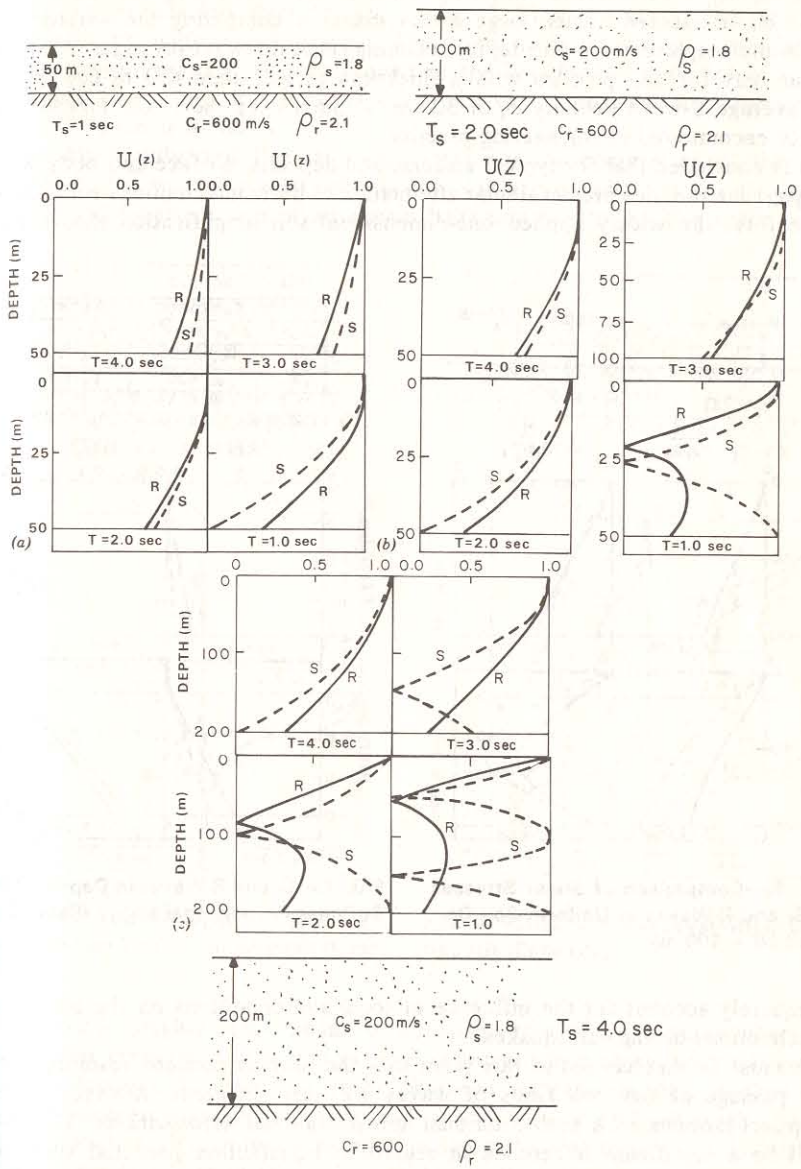

FIG. 5.—Comparison of Displacements of S- and R-Waves in Uniform Soil Deposit on Elastic Bedrock: (*a*) $H = 50$ m; (*b*) $H = 100$ m; (*c*) $H = 200$ m

in a fundamentally different pattern of displacements with depth.

Because R-wave components of periods shorter than 1.5 sec–1.0 sec decay very rapidly with distance (12), only wave periods exceeding 1.0 sec–1.5 sec need be considered. Thus, large errors made in computing the variation of horizontal displacements with depth, assuming vertical S-wave propagation, would occur only for soil profiles with a thickness greater than 450 m–600 m and for average S-wave velocity c_s of 300 m/s. Such deep, soft soil deposits are rarely encountered in engineering practice.

It is concluded that for typical uniform soil deposits, surface and body wave propagation theories predict similar attenuation of horizontal motions with depth. Therefore, the widely applied one-dimensional soil amplification theory may

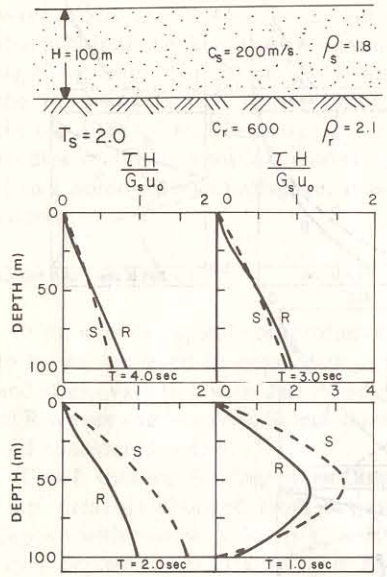

FIG. 6.—Comparison of Shear Stresses of S- and R-Waves in Uniform Soil Deposit (H = 100 m)

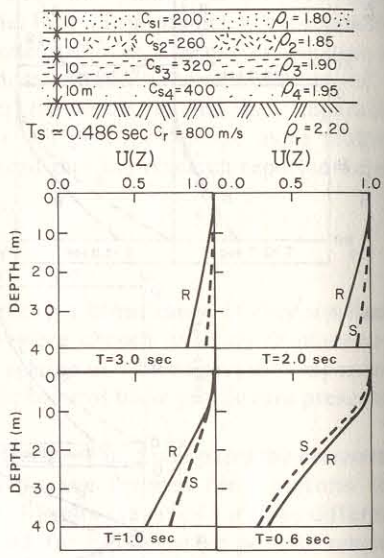

FIG. 7.—S- and R-Waves in Deposit with Stiffness Proportional to $\sqrt{z}$ (Case II)

adequately account for the influence of local soil conditions on the horizontal accelerations during earthquakes.

It must be emphasized at this point that the particle motions resulting from the passage of the two kinds of waves are very different: R-waves induce elliptical motions with both rotational and dilatational deformations. This may well be a significant difference in regard to liquefaction potential since the cyclic shear resistance is different in multidirectional than in unidirectional shaking (14). Moreover, additional rocking and vertical motions are induced by R-waves especially in long, above-ground structures (24).

In addition, when the variation of horizontal shear stresses with depth is considered, the two models may differ considerably, e.g., Fig. 6 shows the relative sensitivity to frequency of the amplitude of shear stresses produced

by vertical S-waves, while the R-wave stress distribution undergoes only minor changes. Notice also that R-waves result in relatively small stresses near the top of the profile. Thus, S-wave theory usually predicts higher stresses at shallow depths for periods less than 3.0 sec in Fig. 6. This is a reversal of what is observed in the halfspace [Fig. 4(*b*)]. Therefore, no definite, general conclusion can be drawn regarding the assessment of the liquefaction potential of a site using the two theories. Rather, each soil profile should be tested for liquefaction due to S-waves or R-waves.

Case II: Multilayered Deposit.—Fig. 7 extends the comparison of the two theories to the case of a relatively shallow soil deposit (H = 40 m) consisting of four soil layers on top of an elastic halfspace (bedrock). The stiffness of

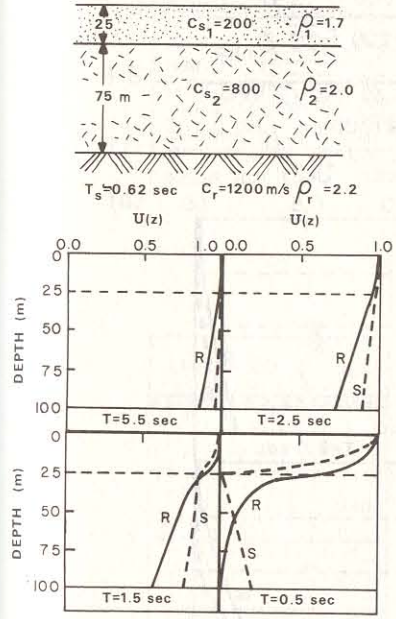

FIG. 8.—S- and R-Waves in "Shallow" Soft Layer on Top of Soil Deposit (Case III)

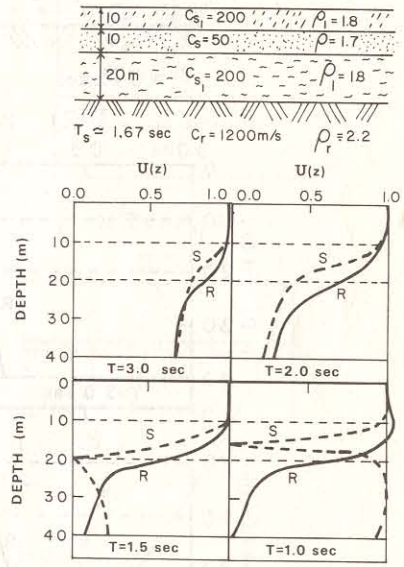

FIG. 9.—Thin, Soft, Soil Layer within Soil Deposit (Case IVa)

each layer is roughly proportional to the square root of the average effective overburden pressure, a situation often encountered in practice with relatively uniform deposits. The general trends observed with the uniform shallow (H = 50 m) deposit (case Ia) are seen with this profile as well, although in this case R-waves result in stronger deamplification with depth throughout the period range of greatest interest (1 sec–3 sec). Again, the differences in the motions induced by the two waves in the upper 10 m of the deposit are negligibly small, and one-dimensional soil amplification theory could be safely used in most geotechnical engineering applications to account for the attenuation of motion with depth of profile.

Case III: "Shallow" Soft Soil Layer on Top of Soil Deposit.—Fig. 8 shows

a comparison of the variation of horizontal displacements with depth for a 25-m-thick soft soil layer having S-wave velocity c_{s1} of 200 m/s and being underlain by a much stiffer soil deposit (c_{s2} = 800 m/s). The differences between the two theories for long periods are minimal and are restricted to the lower part of the profile, (similar to Case II). Again, R-waves result in stronger deamplification than S-waves.

For wave periods as low as 0.5 sec, corresponding to the fundamental natural period of the profile, the two theories predict significantly different amplitudes of motion, particularly at shallow depths. However, the variation of the amplitude

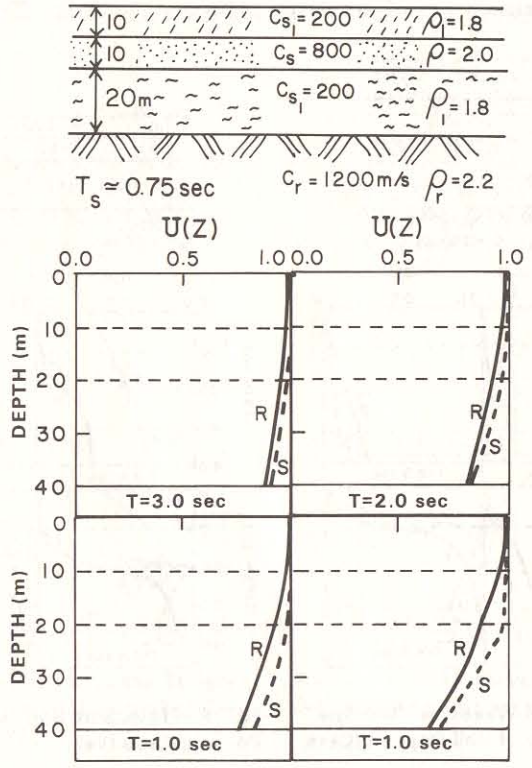

FIG. 10.—Thin, Stiff, Soil Layer within Soil Deposit (Case IVb)

of horizontal motion with depth is similar in its shape and general characteristics for both theories. Insofar as such short period waves do not constitute a significant portion of surface waves, discrepancies between the results of S-wave and R-wave theories at low periods are not of consequence in engineering practice.

Case IV: Thin Soil Layer within Soil Deposit.—A soil deposit (H = 40 m) with a thin, soft or stiff layer (thickness = 10 m) at a shallow depth (10 m below ground surface) has been chosen to further compare the two wave theories. Figs. 9 and 10 give some results of this comparison for a soft (c_s = 50 m/s) and a stiff (c_s = 800 m/s) soil layer, respectively.

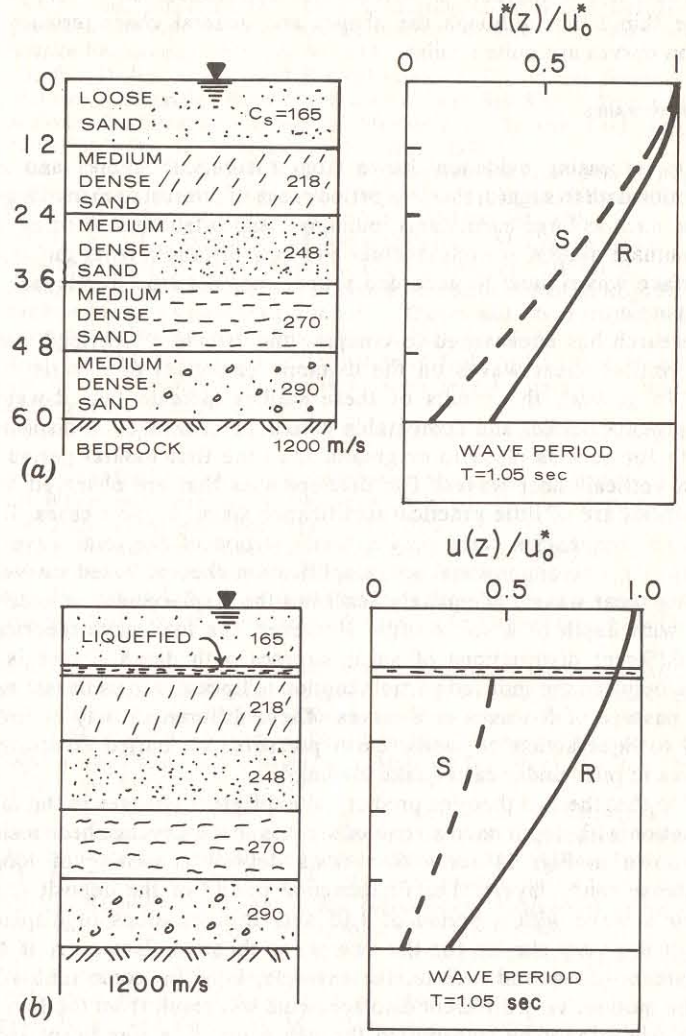

u* displacements before liquefaction occurence

u displacements sufficient time after liquefaction occurence

FIG. 11.—Influence of Liquefied Zone on Displacement Distribution due to S- and R-Waves: (*a*) Displacements before Occurence of Liquefaction; (*b*) Displacements Sufficient Time after Liquefaction Occurence

The predicted displacements show good agreement throughout the period range of interest ($T \geq 1$ sec). The two waves produce nearly identical patterns of displacements above the soft or stiff layers. Differences do occur, however, within the thin layer, although the shapes and general characteristics of the attenuation curves are quite similar.

Concluding Remarks

There is increasing evidence drawn from theoretical studies and existing strong-motion data to suggest that in a period range of interest to many long-period structures, such as large earth dams, buildings, and offshore structures, surface waves dominate motion at both medium and long distances from the epicenter. Thus, surface waves must be accorded proper consideration in relevant studies in soil dynamics.

This research has endeavored to compare the effects of Rayleigh waves to those of vertical shear waves on the dynamic responses of a variety of soil deposits. In general, the results of these studies indicate that R-waves and S-waves produce similar and comparable variations of horizontal displacements with depth for periods close to or greater than the first natural period of the deposit in vertical shear waves. The discrepancies that are observed at much shorter periods are of little practical significance since, in most cases, R-waves of very high frequencies carry only a small portion of the total wave energy (12). Thus, the one-dimensional soil amplification theory, based on vertically propagating shear waves, adequately describes the displacement or acceleration variation with depth of a soil profile. However, the two wave theories seem to yield different distributions of shear stresses with depth. There is also a difference between the induced particle motion (elliptical versus linear) resulting from the passage of R-waves or S-waves. These differences may be important in regard to liquefaction of sands, earth pressures on buried structures, and the stresses in piles under earthquake loadings.

Note also that the two theories predict quite different changes in the displacement variation with depth once a zone of soil has lost its cyclic shear resistance. This is shown in Fig. 11 for a 60-m-thick deposit consisting of loose and medium-dense sandy layers. The fundamental period of the deposit is approx 1 sec. For a wave with a period of 1.05 sec, the variations of displacement with depth are very similar for the two wave theories. However, if the soil mass between -11 m and -12 m, for example, liquefies some time after the start of the motion, very different displacements will result from the two waves. Since S-waves cannot be transmitted through a liquid, a significant reduction will result in the displacements of the lower 48 m of the deposit, whose natural period is 0.8 sec. In other words, the resonance phenomenon for the S-waves dies away as soon as liquefaction occurs. However, the R-wave-induced motions remain almost unaffected from the liquefaction occurrence.

Appendix I.—References

1. Anderson, J., "A dislocation Model for the Parkfield Earthquake," *Bulletin of the Seismological Society of America,* Vol. 64, 1974, pp. 671–686.
2. Cherry, S., "Estimating Underground Motions from Surface Accelerograms," *Engineering Seismology and Earthquake Engineering,* J. Solnes, ed., 1974.
3. Ewing, Jardesky, and Press, "*Elastic Waves in Layered Media,*" McGraw Hill Book Co., Inc., New York, N.Y., 1957.
4. Gazetas, G., and Bianchini, G., "Field Evaluation of Body and Surface-Wave Soil Amplification Theories," *Proceedings,* Second United States National Conference on Earthquake Engineering, 1979, pp. 603–613.
5. Hall, J. R., Shulka, D. K., and Kissepfenning, J. F., "Shear Stress Distribution Due to Shear and Rayleigh Wave Propagation at Deep Soil Sites," *Proceedings,* Fourth International Conference on Structural Mechanics in Reactor Technology, Vol. K (a), Paper No. 1/15, San Francisco, Calif., Aug., 1977.
6. Harkrider, D. G., "Surface Waves in Multilayered Elastic Media I: Rayleigh and Love Waves from Buried Sources in a Multilayered Elastic Halfspace," *Bulletin of the Seismological Society of America,* Vol. 54, 1964, pp. 627–679.
7. Haskell, N. A., "The Dispersion of Surface Waves in Multilayered Media," *Bulletin of the Seismological Society of America,* Vol. 65, 1960, pp. 4147–4150.
8. Hermann, R. B., and Nuttli, O. W., "Ground Motion Modelling at Regional Distances for Earthquakes in a Continental Interior, I. Theory and Observations," *Earthquake Engineering and Structural Dynamics,* Vol. 4, 1975, pp. 49–58.
9. Liang, G. C., and Duke, C. M., "Separation of Body and Surface Waves in Strong Ground Motion Records," *Proceedings,* Sixth World Conference on Earthquake Engineering, New Delhi, India, 1977.
10. Lysmer, J., "Lumped Mass Method for Rayleigh Waves," *Bulletin of the Seismological Society of America,* Vol. 60, 1970, p. 89.
11. Lysmer, J., and Drake, L. A., "A Finite Element Method for Seismology," *Seismology: Surface Waves and Earth Oscillations,* B. A. Bolt, ed., Vol. 11, Methods in Computational Physics Series, Academic Press, N.Y., 1972.
12. Lysmer, J., "Analytical Procedures in Soil Dynamics," *Proceedings of the Specialty Conference on Soil Dynamics and Earthquake Engineering,* ASCE, 1978, pp. 1267–1316.
13. Nemani, D., and Mal, A. K., "Short Period Surface Waves in a Layered Medium," *Proceedings,* Sixth World Conference on Earthquake Engineering, New Delhi, India, 1977.
14. Pyke, R. M., Chan, C. K., and Seed, H. B., "Settlement and Liquefaction of Sands under Multi-Directional Shaking," *Report No. EERC 74-2,* Earthquake Engineering Research Center, University of California, Berkeley, Calif., Feb., 1974.
15. Roesset, J. M., "Soil Amplification of Earthquakes," *Numerical Methods in Geotechnical Engineering,* Desai and Christian, eds., McGraw-Hill, Book Co., Inc., New York, N.Y., 1977, pp. 639–682.
16. Seed, H. B., "The Influence of Local Soil Conditions on Earthquake Damage," *Proceedings,* Soil Dynamics Specialty Session, Seventh International Conference of Soil Mechanics and Foundation Engineering, Mexico City, Mexico, 1969.
17. Seed, H. B., Lysmer, J., and Huang, R., closure to "Soil-Structure Interaction Analysis for Seismic Response," *Journal of the Geotechnical Engineering Division,* ASCE, Vol. 103, No. GT4, Proc. Paper 12831, Apr., 1977, pp. 341–346.
18. Seed, H. B., and Idriss, I. M., "Simplified Procedure for Evaluating Soil Liquefaction Potential," *Journal of Soil Mechanics and Foundations Division,* ASCE, Vol. 97, No. SM9, Proc. Paper 8371, Sept., 1971, pp. 1249–1273.
19. Swanger, H. J., and Boore, D. M., "Simulation of Strong Motion Displacements Using Surface-Wave Modal Superposition," *Bulletin of the Seismological Society of America,* Vol. 68, No. 4, Aug., 1978, pp. 907–922.
20. Thomson, W. T., "Transmission of Elastic Waves through a Stratified Soil Medium," *Journal of Applied Physics,* Vol. 21, Feb., 1950.
21. Toki, K., "Disintegration of Accelerograms into Surface and Body Waves," *Proceedings,* Sixth World Conference on Earthquake Engineering, New Delhi, India, 1977.
22. Trifunac, M. D., "A Three-Dimensional Dislocation Model for the San Fernando Earthquake of February 9, 1971," *Bulletin of the Seismological Society of America,* Vol. 64, 1974, pp. 149–172.
23. Trifunac, M. D., "Response Spectra of Earthquake Ground Motion," *Journal of the Engineering Mechanics Division,* ASCE, Vol. 104, No. EM5, Proc. Paper 14051, Oct., 1978, pp. 1081–1093.
24. Wong, H. L., and Luco, J. E., "Dynamic Response of Rectangular Foundations

to Obliquely Incident Waves," *Earthquake Engineering and Structural Dynamics*, Vol. 6, 1978, pp. 3–16.

Appendix II.—Notation

The following symbols are used in this paper:

A', A'', B', B'' = wave amplitudes in Eqs. 2, 5, and 8;
c = horizontal phase velocity;
c_p = P-wave velocity;
c_R = R-wave velocity;
c_s = S-wave velocity;
G = shear modulus;
H = depth of soil deposit to rock (in Fig. 6);
h = focal depth (Eq. 1);
k = wave number;
R = epicentral distance in Eq. 1, also indicates R-wave curves in Figs. 4–11;
S = S-wave curves in Figs. 4–11;
T = period of harmonic waves;
T_s = fundamental period of soil deposit in vertical S-waves;
t = time;
U = u/u_0 = normalized horizontal displacement;
u = horizontal displacement;
u_0 = horizontal displacement at surface;
W = w/w_0 = normalized vertical displacement;
w = vertical displacement; w_0 = vertical displacement at the surface;
ϵ = dilatation (defined in Eq. 2*a*);
θ = angle of incidence with respect to the vertical direction);
λ = wave length;
ν = Poisson's ration;
ρ = mass density (in grams/cubic centimeter);
σ = normal stress;
τ = shear stress;
Ω = rotation (defined in Eq. 2*b*); and
ω = angular frequency.

Subscripts

R = R-wave; and
S = S-wave.

JOURNAL OF THE GEOTECHNICAL ENGINEERING DIVISION

Seismically Induced Sliding of Massive Structures[a]

By Eduardo A. Kausel,[1] A. M. ASCE, A. Stanley Lucks,[2] M. ASCE, Lewis Edgers,[3] A. M. ASCE, William F. Swiger,[4] F. ASCE, and John T. Christian,[5] M. ASCE

Introduction

The classical, pseudostatic limiting equilibrium analysis for the sliding stability of structures during seismic events gives factors of safety against sliding that appear unrealistically low in many cases. Further, these methods provide no information on the actual magnitude of sliding motions, should they occur. The classical analysis is shown in Fig. 1. Horizontal and vertical forces due to seismic effects are computed by adding the products of mass times peak acceleration throughout the structure. These forces are then treated as static loads that, in combination with the weight of the structure and other forces such as those due to lateral soil and water pressures, must be resisted by the soil. The result of the analysis is expressed as a factor of safety defined as the ratio of resisting forces to the driving forces.

Newmark (1965) in his Fifth Rankine Lecture "Effects of Earthquakes on Dams and Embankments," developed a means of estimating the amount of displacement of a rigid block subjected to seismic excitations and driven by Coulomb friction at the block-foundation interface. The method was developed for slopes and dames, but the procedure can be applied to other types of structures.

Note.—Discussion open until May 1, 1980. To extend the closing date one month, a written request must be filed with the Editor of Technical Publications, ASCE. This paper is part of the copyrighted Journal of the Geotechnical Engineering Division, Proceedings of the American Society of Civil Engineers, Vol. 105, No. GT12, December, 1979. Manuscript was submitted for review for possible publication on May 16, 1976.

[a]Presented at the April 2–6, 1979, ASCE Convention & Exposition and Continuing Education Program, held at Boston, Mass. (Preprint 3595).

[1]Assoc. Prof. of Civ. Engrg., Massachusetts Inst. of Tech., Cambridge, Mass.; also, Consultant, Stone & Webster Engrg. Corp., Boston, Mass.

[2]Chf. Geotechnical Engr., Stone & Webster Engrg. Corp., Boston, Mass.

[3]Assoc. Prof. of Civ. Engrg., Tufts Univ., Medford, Mass.; also, Consultant, Stone & Webster Engrg. Corp., Boston, Mass.

[4]Vice Pres. and Sr. Consulting Engr., Stone & Webster Engrg. Corp., Boston, Mass.

[5]Consulting Engr., Stone & Webster Engrg. Corp., Boston, Mass.